Bull. Chem. Soc. Ethiop. **2024**, 38(2), 431-443.
DOI: https://dx.doi.org/10.4314/bcse.v38i2.11

ISSN 1011-3924
Printed in Ethiopia
Online ISSN 1726-801X

CAPTURING OF THE COPPER(II) IONS BY SEVERAL 4-AMINOANTIPYRINE SCHIFF BASES: SYNTHESIS, SPECTROSCOPIC ANALYSIS, AND DECOMPSITION OF THE RESULTED COMPLEXES INTO COPPER(II) OXIDE

Samar O. Aljazzar*

Department of Chemistry, College of Science, Princess Nourah bint Abdulrahman University, P.O. Box 84428, Riyadh 11671, Saudi Arabia

(Received December 4, 2023; Revised December 23, 2023; Accepted December 25, 2023)

ABSTRACT. Here we describe the synthesis and characterization of three Schiff bases based on 4-aminoantipyrine, ligand A, ligand B, and ligand C. Ligand A was synthesized by reacting 4-aminoantipyrine with hydrazine, ligand B by reacting 4-aminoantipyrine with ethylenediamine, and ligand C by reacting 4-aminoantipyrine with benzaldehyde and hydrazine. The synthesis of the desired Schiff base derivatives was successfully achieved, as confirmed by elemental analysis, Fourier-transform infrared (FT-IR) spectroscopy, and nuclear magnetic resonance (^{1}H and ^{13}C NMR) spectroscopy. The obtained experimental results exhibited excellent agreement with previously published data. To evaluate the reactivity of the synthesized Schiff bases in forming stable metal complexes, their reaction with copper(II) ions was examined. The results indicated that ligand A and ligand B effectively utilized the four nitrogen atoms (NNNN) from the 4-aminoantipyrine-N and azomethine-N groups to coordinate with copper(II) ions, while ligand C coordinated with the copper(II) ions using its four azomethine nitrogen atoms. Furthermore, the manufactured copper(II) complexes were subjected to thermal treatment in the air at 600 °C for 3 h, resulting in the successful generation of copper(II) oxide. Scanning electron microscopy-energy-dispersive X-ray analysis data demonstrated that the produced copper(II) oxide exhibited high purity and possessed a uniform and well-structured morphology.

KEY WORDS: Schiff bases, 4-Aminoantipyrine, Copper(II) ion, Thermal decomposition, SEM/EDX, Morphology

INTRODUCTION

Copper plays a diverse role in biological systems and has been extensively investigated in relation to various human diseases from medicinal and biochemical perspectives [1]. Studies have explored the antibacterial and antiviral activities of copper-based compounds and their potential chemotherapeutic properties. Furthermore, the biochemical interactions between copper-based compounds and non-steroidal anti-inflammatory drugs, as well as the cytotoxic activity of copper-based compounds through enzyme inhibition or induction of cell apoptosis, have been thoroughly reviewed [2]. On the other hand, nano-copper(II) oxide has emerged as a new generation of environmentally friendly catalysts with broad potential applications in the field of environmental protection. Copper(II) oxide exhibits remarkable properties, including its abundance in natural raw materials, non-toxic nature, and cost-effective production processes. These desirable characteristics enable the utilization of copper(II) oxide in electronic and optoelectronic devices such as nanocatalysis devices, field emitters, solar cells, gas sensors, electrochemical cells, and magnetic storage media [3]. One important class of organic compounds is Schiff bases, which are derived from the reaction between an aldehyde or a ketone and a primary amine. In this reaction, the carbonyl group (–C=O) of the aldehyde or ketone is replaced by an imine (>C=N–) or azomethine (–CH=N–) group [4]. Several Schiff bases exhibit structural similarities to natural biological substances [5]. Their applications extend beyond the preparation of inorganic and organic compounds, finding diverse uses in the medicinal, pharmaceutical, agricultural, catalytic, and industrial fields [6-9]. Numerous metal complexes of Schiff bases have exhibited significant

*Corresponding author. E-mail: drsamaraljazzar2020@gmail.com; soaljazar@pnu.edu.sa

biological properties, such as anti-tumor, antibacterial, anti-carcinogenic, and fungicidal activities. Additionally, they have been employed as polymer stabilizers, pigment dyes, intermediates in organic synthesis, catalysts in various biological systems, and tools for analyzing pharmacological constituents [10, 11]. 4-Aminoantipyrine is a derivative of antipyrine that features a phenyl ring connected to a pyrazolone moiety, which is a five-membered heterocyclic ring containing adjacent nitrogen atoms, a carbonyl group, and an amino group. Due to its multiple donor sites, 4-aminoantipyrine can be employed to synthesize Schiff bases capable of binding metal ions. This study specifically focuses on synthesizing three 4-aminoantipyrine-based Schiff bases that offer four nitrogen atoms (NNNN) as coordination sites for capturing copper(II) ions. These Schiff bases are referred to as ligand A, obtained through the reaction of 4-aminoantipyrine with hydrazine; ligand B, obtained through the reaction of 4-aminoantipyrine with ethylenediamine; and ligand C, obtained through the reaction of 4-aminoantipyrine with benzaldehyde and hydrazine. Finally, the manufactured copper(II) complexes were subjected to thermal treatment in the air at 600 °C for 3 h, resulting in the successful generation of copper(II) oxide.

EXPERIMENTAL

Chemicals

Analytical grade 4-amino-2,3-dimethyl-1-phenyl-3-pyrazolin-5-one (4-aminoantipyrine; $C_{11}H_{13}N_3O$; 203.24 g/mol), hydrazine solution (NH_2NH_2; 32.05 g/mol), 1,2-diaminoethane (ethylenediamine; $NH_2CH_2CH_2NH_2$; 60.10 g/mol), benzaldehyde (C_6H_5CHO; 106.12 g/mol), and copper(II) chloride ($CuCl_2$; 134.45 g/mol) were provided by Fluka Company (Seelze, Germany) and BDH Chemicals (UK).

Manufacturing of the Schiff base derivatives

Ligand A. Ligand A is a Schiff base with the IUPAC name 3,3'-(hydrazine-1,2-diylidene)bis(-4-amino-1,5-dimethyl-2-phenyl-2,3-dihydro-1H-pyrazole). It was prepared following previously described methods [12-15]. To prepare ligand A, 2 mmol of 4-aminoantipyrine dissolved in 25 mL of MeOH solvent was mixed with 1 mmol of hydrazine dissolved in 25 mL of MeOH solvent. The mixture was refluxed on a hot plate at 60 ºC for 2 h. The resulting yellow-orange-colored precipitates were filtered from the system and thoroughly washed with MeOH and EtOEt. The product was then re-crystallized in MeOH and dried in a drying pot over calcium chloride for 48 h. Ligand A yielded 63% of the expected amount, had a melting point of 180°C, and its chemical structure is shown in Figure 1.

Ligand B. Ligand B is a Schiff base with the IUPAC name 3,3'-(ethane-1,2-diylbis(azaneylylidene))bis(4-amine-1,5-dimethyl-2-phenyl-2,3-dihydro-1H-pyrazole). It was prepared using a procedure like that reported in the literature [12-15]. To prepare ligand B, 2 mmol of 4-aminoantipyrine dissolved in 25 mL of MeOH solvent was mixed with 1 mmol of ethylenediamine dissolved in 25 mL of MeOH solvent. The mixture was refluxed on a hot plate at 60 ºC for 2 h. The resulting, yellow-colored precipitates were filtered from the system and thoroughly washed with MeOH and EtOEt. The product was then re-crystallized in MeOH and dried in a drying pot over calcium chloride for 48 h. Ligand B yielded 62% of the expected amount, had a melting point of 220 °C, and its chemical structure is presented in Figure 1.

Ligand C. Ligand C is a Schiff base with the IUPAC name *N*,*N'*-(hydrazine-1,2-diylidenebis(1,5-dimethyl-2-phenyl-2,3-dihydro-1*H*-pyrazole-4-yl-3-ylidene))bis(1-phenylmethan-imine). It was prepared using a procedure reported in the literature [12-15] in two stages. In the first stage, 1 mmol of 4-aminoantipyrine dissolved in 25 mL of MeOH solvent was mixed with 1 mmol of

benzaldehyde dissolved in 25 mL of MeOH solvent. The mixture was continuously stirred for 2 h under gentle heat. Pale-yellow-colored precipitates were formed, which were then filtered, washed, re-crystallized in MeOH, and oven-dried at 70 ºC. In the second stage, 2 mmol (in 25 mL MeOH) of the resulting pale-yellow product was refluxed with 1 mmol (in 25 mL MeOH) of hydrazine at 60 ºC for 2 h on a hot plate. The refluxed mixture was then poured into a 250-mL beaker containing crushed ice. This generated ligand C as a brownish-yellow-colored product, which was filtered, thoroughly washed with MeOH, re-crystallized, and dried in a drying pot over calcium chloride for 48 h. Ligand C yielded 65% of the expected amount, had a melting point of 195 °C, and its chemical structure is provided in Figure 1.

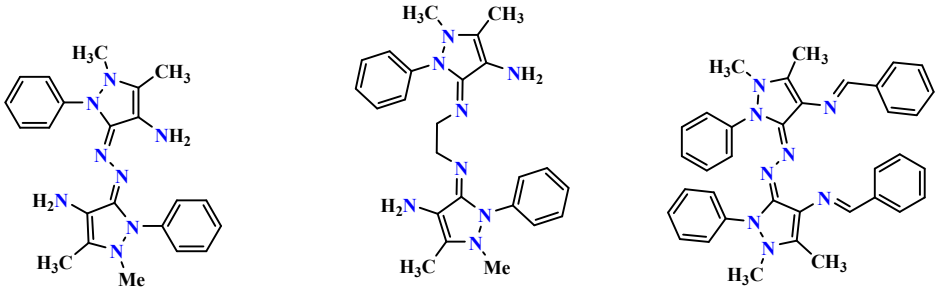

Figure 1. Chemical structures of the synthesized ligands (A, B, and C).

Schiff base copper complexes

The molar ratio of the copper ion interaction with the Schiff base is 1:1. Three individual methanolic solutions (50 mL each) containing 2 mmol of ligand A, ligand B, and ligand C were prepared and stirred on a multi-position hotplate stirrer at 60 °C. Gradually, a 50 mL aqueous solution of copper(II) chloride (2 mmol) was added to each ligand solution. The three mixtures were stirred for an additional 10 min and then transferred to refluxing systems. After 2 h of refluxing at 60 °C under continuous stirring, the mixture solutions containing visible bluish-black-colored precipitates were transferred into 250-mL beakers. The mixture solutions were reduced to one-half by evaporating on a water bath, resulting in the formation of dense bluish-black-colored products in each beaker. The formed copper(II) complexes were filtered off and washed several times with MeOH and EtOEt solvents. To enhance the purity of the manufactured copper(II) complexes, they were re-crystallized from MeOH, collected, and finally oven-dried at 70 °C. The copper(II) complex obtained with ligand A was termed complex A, the one obtained with ligand B was termed complex B, and the last one was termed complex C.

Copper(II) oxide

Complex A, complex B, and complex C (5 g) were subjected to calcination in an electric furnace at 600 °C for 3 h in the presence of air. This process resulted in the decomposition of the copper(II) complexes, producing copper(II) oxides. Samples of the manufactured copper(II) oxides were analyzed for their FT-IR spectra using a Bruker ALPHA compact FT-IR spectrophotometer. Elemental analyses and information regarding the structural morphology were obtained through scanning electron microscopy-energy dispersive X-ray analysis (SEM/EDX) data collected using a JSM-6390LA JEOL (Tokyo, Japan) integrated with a JED-2300 EDXRF spectrometer.

RESULTS AND DISCUSSION

Manufactured ligands

Ligand A. Table 1 lists the elemental percentages (%) of C, H, and N in the ligands A, B, and C. A sample of ligand A gives the following results: Yellow-orange-colored powder; yield 63%; IR data (cm^{-1}): 3437, 3329, 2997, 2914, 1656, 1594, 1510, 1448, 1364, 1280, 1190, 1125, 750, 580. ^{1}H NMR chemical shifts (400 MHz, DMSO-d_6) were: δ = 7.51 (m, 6H, phenyl), 7.28 (m, 4H, phenyl), 3.42 (s, 4H, $2NH_2$), 2.77 (s, 6H, $2NCH_3$), 2.13 (s, 6H, $2CH_3$). ^{13}C NMR chemical shifts (100 MHz, DMSO-d_6) were: δ= 161.4, 135.5, 128.8, 125.1, 121.8, 120.0 (C=C, C=N, C=C, C-N), 40.1, 9.8 ($2CH_3$).

Ligand A has two amino groups ($-NH_2$), which generate several FT-IR spectral bands due to the different modes of vibrations. These bands were resonated at 3437 and 3329 cm^{-1} due to the $\nu(NH_2)$ vibration, at 1656 cm^{-1} due to the $\delta_{def}(NH_2)$ vibration, and at 1364 cm^{-1} due to the $\delta_{wag}(NH_2)$ vibration. The twisting and rocking vibrations of $-NH_2$ groups were observed at lower frequencies, 1125 cm^{-1} and 580 cm^{-1}, respectively. Ligand A also displayed IR absorption bands at 1594, 1510, and 1448 cm^{-1} which could be assigned to the ν(C=N), ν(C=C), and $\delta_{sciss}(CH_3)$ vibrations, respectively. The bands located at 1280 and 1190 cm^{-1} could be referred to as the ν_{asym}(C-N) and ν_{sym}(C-N) vibrations, respectively. The ^{1}H NMR spectrum of ligand A collected at room temperature in DMSO-d_6 solvent produced five signals of proton resonances. The ten aromatic protons from the phenyl rings resonated in the region 7.28–7.51 ppm. The four protons of the ($-NH_2$) groups display a singlet signal at 3.42 ppm. The six protons from the $-NCH_3$ moieties resonated as a sharp singlet at 2.77 ppm. The ^{13}C NMR spectrum of Ligand A displayed eight resolved carbon signals in the δ = 9.8–161.4 ppm range. The elemental and spectral data (FT-IR, ^{1}H and ^{13}C NMR) of ligand A agreed well with those previously reported [12-15], confirming that we successfully synthesized ligand A.

Table 1. The elemental percentages (%) of C, H, and N in the ligands A, B, and C.

Ligand	C %		H %		N %	
	Observed	Calculated	Observed	Observed	Observed	Calculated
Ligand A	65.37	65.59	6.65	6.46	27.60	27.83
Ligand B	66.65	66.89	7.10	6.97	25.88	26.01
Ligand C	74.77	74.69	6.10	5.88	19.19	19.36

Ligand B. A sample of ligand B gives the following results: Yellow-colored powder; yield 62%; IR data (cm^{-1}): 3435, 3324, 2998, 2910, 1648, 1592, 1496, 1452, 1414, 1355, 1273, 1230, 1190, 1116, 925, 756, 665, 572. ^{1}H NMR chemical shifts (400 MHz, DMSO-d_6) were: δ = 7.40 (m, 8H, phenyl), 7.21 (t, 2H, phenyl), 3.99 (b, 4H, $2NH_2$), 2.74 (s, 6H, $2NCH_3$), 2.1 (s, 4H, $2CH_2$), and 1.77 (s, 6H, $2CH_3$). ^{13}C NMR chemical shifts (100 MHz, DMSO-d_6) were: δ = 174.2, 169.8, 161.8, 136.0, 129.6, 125.6, 122.3, 120.5 (C=C, C=N, C=C, C-N), 38.73 ($2CH_2$), 23.76, 10.35 ($2CH_3$).

The two amino groups ($-NH_2$) in ligand B absorb across a wide range of FT-IR frequencies from 3435 to 572 cm^{-1}. The different vibrational modes of $-NH_2$: $\nu(NH_2)$, $\delta_{def}(NH_2)$, $\delta_{wag}(NH_2)$, $\delta_{twist}(NH_2)$, and $\delta_{rock}(NH_2)$ are responsible for the FT-IR bands located at (3435 and 3324), 1648, 1355, 1116, and 572 cm^{-1}, respectively. The FT-IR absorption bands at 1592 cm^{-1} are due to the ν(C=N) vibrations, 1496 cm^{-1} from the ν(C=C) vibrations, 1452 and 1414 cm^{-1} from the scissoring modes of $-CH_3$ and $-CH_2$, respectively, and 1273 and 1190 cm^{-1} from the asymmetric and symmetric vibrations of the C-N bonds, respectively. The ^{1}H NMR spectrum of ligand B showed that it produced 28 protons, which appeared in the δ = 1.77–7.40 ppm range. The ten aromatic protons from the phenyl rings resonated in the region 7.21–7.40 ppm. The four protons of the ($-NH_2$)

groups display a broad signal at 3.99 ppm. The six protons from the -NCH_3 moieties resonated as a sharp singlet at 2.10 ppm. The ^{13}C NMR spectrum of Ligand B showed that it produced 11 carbon resonances. These carbon signals were observed with the region of δ = 10.35–174.2 ppm. The obtained FT-IR, ^1H and ^{13}C NMR spectral results for ligand B are in good agreement with those previously reported [12-15] and confirmed that we successfully synthesized ligand B.

Ligand C. A sample of ligand C produces the following results: Brownish-yellow-colored powder; yield 65%; IR data (cm^{-1}): 3036, 2933, 2850, 1650, 1565, 1487, 1447, 1378, 1304, 1129, 874, 757, 695. ^1H NMR chemical shifts (400 MHz, DMSO-d_6) were: δ = 9.62 (s, 2H, -N=CH-), 7.39-8.73 (m, 20H, phenyl), 3.18-3.42 (s, 6H, $2NCH_3$), 2.11 (s, 6H, 2CH). ^{13}C NMR chemical shifts (100 MHz, DMSO-d_6) were: δ = 161.4, 154.4, 152.1, 137.5, 134.5, 130.1, 128.6, 124.6, 116.3 (C=C, C=N, C=C, C-N), 38.5, 9.7 ($2CH_3$).

The FT-IR absorption bands resonated at 1650 cm^{-1} due to the ν(–CH=N) vibrations, 1565 cm^{-1} from the ν(–C=N–N) vibrations, 1447, 1378, 757, and 695 cm^{-1} from the scissoring, rocking, wagging, and twisting modes of -CH_3, respectively, and 1304 and 1129 cm^{-1} from the asymmetric and symmetric vibrations of the C-N bonds, respectively. The protons of the azomethine (–CH=N) groups were responsible for the singlet signal appearing at δ 9.62 ppm in the ^1H NMR spectrum of ligand C. The six protons of the -NCH_3 moieties generated signals in the range δ 3.18–3.42 ppm. Ligand C possesses four phenyl rings containing 20 aromatic protons producing signals within the region from 7.39 to 8.73 ppm. The ^{13}C NMR spectrum of ligand C showed that it produced 11 carbon resonances. These resolved carbon signals were observed with the region of δ = 9.7–161.4 ppm. The experimental FT-IR, ^1H and ^{13}C NMR data for ligand C agree with those previously reported [12-15] and confirmed that we successfully synthesized ligand C.

Capturing of the copper(II) ions

Compositions

The synthesized ligands were used to capture copper(II) ions from aqueous media. The reaction of ligand A, ligand B, and ligand C with copper(II) ions at 60 °C resulted in the formation of black-colored complexes. The obtained copper(II) complexes were purified, re-crystallized, and analyzed to determine their compositions, including the content of C, H, N, and copper. The copper content was determined using a gravimetric technique, while the content of C, H, and N elements was determined using a CHN elemental analyzer. The copper(II) complex formed with ligand A is referred to as complex A, the one formed with ligand B is referred to as complex B, and the complex formed with ligand C is referred to as complex C. Complex A, complex B, and complex C were obtained with percentage yields of 63%, 65%, and 63%, respectively, with melting points above 250 °C. Table 2 lists the elemental percentages (%) of C, H, and N in the complexes A, B, and C. The data in Table 2 indicate that the reaction stoichiometry is 1:1 (ligand to copper) and comply with the suggested general compositions of $[Cu(ligand)]Cl_2$.

FT-IR analysis

The synthesized copper(II) complexes were subjected to the FT-IR analysis, and the collected spectra are presented in Figure 2. The IR spectral data collected for the synthesized copper(II) complexes were: Complex A: 3245 and 3192 cm^{-1} $\nu(NH_2)$, 3050 cm^{-1} ν_{asym}(C-H), 2926 cm^{-1} ν_{sym}(C-H), 1640 cm^{-1} $\delta_{def}(NH_2)$, 1580 cm^{-1} ν(C=N), 1488 cm^{-1} ν(C=C), 1448 cm^{-1} $\delta_{sciss}(CH_3)$, 1411 cm^{-1} $\delta_{wag}(NH_2)$, 1303 cm^{-1} ν_{asym}(C-N), 1170 cm^{-1} ν_{sym}(C-N), 1115 cm^{-1} $\delta_{twist}(NH_2)$, 1022 cm^{-1} $\delta_{wag}(CH_3)$, 885 cm^{-1} δ_{def}(C-H), 755 cm^{-1} ($\delta_{twist}CH_3$), 635 cm^{-1} $\delta_{rock}(NH_2)$, and 496 cm^{-1} ν(Cu-N).

Table 2. The elemental percentages (%) of C, H, N and Cu in the complexes A, B, and C.

Complex	C %		H %		N %		Cu %	
	Observed	Calculated	Observed	Observed	Observed	Calculated	Observed	Calculated
Complex A	48.95	49.17	4.95	4.84	20.70	20.86	12.05	11.84
Complex B	50.70	50.97	4.87	5.32	19.97	19.82	11.13	11.25
Complex C	60.72	60.60	5.00	4.77	15.55	15.71	9.09	8.91

Complex B. 3240 and 3155 cm^{-1} $\nu(NH_2)$, 3037 cm^{-1} ν_{asym}(C-H), 2942 cm^{-1} ν_{sym}(C-H), 1680 cm^{-1} $\delta_{def}(NH_2)$, 1578 cm^{-1} ν(C=N), 1490 cm^{-1} ν(C=C), 1444 cm^{-1} $\delta_{sciss}(CH_3)$, 1410 cm^{-1} $\delta_{sciss}(CH_2)$, 1396 cm^{-1} $\delta_{wag}(NH_2)$, 1297 cm^{-1} $\delta_{rock}(CH_2)$, 1200 cm^{-1} ν_{asym}(C-N), 1146 cm^{-1} ν_{sym}(C-N), 1105 cm^{-1} $\delta_{twist}(NH_2)$, 915 cm^{-1} $\delta_{wag}(CH_3)$, 830 cm^{-1} δ_{def}(C-H), 755 cm^{-1} ($\delta_{twist}CH_3$), 690 cm^{-1} $\delta_{twist}(CH_2)$, 583 cm^{-1} $\delta_{rock}(NH_2)$, and 500 cm^{-1} ν(Cu-N). Complex C: 3050 cm^{-1} ν_{asym}(C-H), 2926 cm^{-1} ν_{sym}(C-H), 1665 cm^{-1} ν(–CH=N), 1592 cm^{-1} ν(–C=N–N), 1490 cm^{-1} ν(C=C), 1447 cm^{-1} $\delta_{sciss}(CH_3)$, 1405 cm^{-1} $\delta_{rock}(CH_3)$, 1352 cm^{-1} ν_{asym}(C-N), 1168 cm^{-1} ν_{sym}(C-N), 884 cm^{-1} δ_{def}(C-H), 755 cm^{-1} $\delta_{wag}(CH_3)$, 690 cm^{-1} $\delta_{twist}(CH_3)$, and 497 cm^{-1} ν(Cu-N). Most of the main FT-IR features of the free ligands (A, B, and C) were observed in the FT-IR spectra of the corresponding copper(II) complexes. Several of these absorption bands show changes in the profile and position. After the formation of Complex A, the position of the characteristics vibrational modes of -NH_2 groups resulted from the $\nu(NH_2)$, $\delta_{def}(NH_2)$, $\delta_{wag}(NH_2)$, $\delta_{twist}(NH_2)$, and $\delta_{rock}(NH_2)$ vibrations moving from (3437 and 3329) 1656, 1364, 1125, and 580 cm^{-1}, respectively, in the free ligand A to (3245 and 3192) 1640, 1411, 1115, and 635 cm^{-1}, respectively, in complex A. In ligand B, these vibrational modes were moved from (3435 and 3324), 1648, 1355, 1116, and 572 cm^{-1}, to (3240 and 3155), 1680, 1396, 1105, and 583 cm^{-1}, respectively, in complex B. The absorption band due to the vibration of ν(C=N), which was observed at 1594 cm^{-1} and 1592 cm^{-1} in the FT-IR spectra of free ligand A and ligand B, respectively, was shifted to lower frequencies in complex A and complex B and appeared at 1580 cm^{-1} and 1578 cm^{-1}, respectively. The new low-to-medium intensity bands observed at 496 cm^{-1} for complex A and at 500 cm^{-1} from complex B, could be attributed to the stretching vibrations of the copper-nitrogen bond; ν(Cu-N) [16]. Complexation of Ligand C with copper(II) ions shifted the characteristic absorption bands of ν(C=N) vibrations from the (–CH=N) and (–C=N–N) moieties from 1650 and 1565 cm^{-1} in free ligand C to 1665 and 1592 cm^{-1} in complex C, respectively. Also, the complexation generates a low-intensity absorption band resonated at 497 cm^{-1} in the FT-IR spectrum of complex C, which could be referred to as the ν(Cu-N) vibrations. In general, the characteristic FT-IR spectral shifts suggested that ligand A and ligand B effectively utilized the four nitrogen atoms (NNNN) of the 4-aminoantipyrine-N and azomethine-N groups to catch copper(II) ions, while ligand C binds to the copper(II) ions using the four azomethine nitrogen atoms (NNNN). The proposed chemical structures of the synthesized copper(II) complexes are presented in Figure 3.

Decomposing the copper complexes

EDX data

The manufactured copper(II) complexes were subjected to thermal treatment in the air at 600 °C for a duration of 3 h, resulting in the formation of copper(II) oxide (CuO). The oxide derived from complex A is referred to as oxide A, the one from complex B is referred to as oxide B, and that produced by complex C as oxide C. The elemental composition of the manufactured oxides (A, B, and C) was verified using EDX spectra, which were scanned using a JED-2300 EDXRF spectrometer and are presented in Figure 4. The spectra confirmed the presence of four peaks with different intensities, with three peaks corresponding to the copper element and a single peak

indicating the presence of oxygen at 0.525 keV. The strongest copper peak was observed at 8.040 keV (Ka). The EDX spectrum of oxide C also exhibited an additional peak at approximately ~0.25 keV, which can be attributed to the carbon element, indicating that oxide C was contaminated with some residual carbons. The elemental compositions of oxide A, oxide B, and oxide C were determined to be (Cu 79.60% and O 20.40%), (Cu 80.15% and O 19.85%), and (Cu 77.65%, O 18.35%, and C 4.0%), respectively. Oxide A and oxide B exhibited high purity, as their compositions were in excellent agreement with the corresponding theoretical values (Cu 79.89% and O 20.11%) calculated from the chemical formula of CuO (79.55 g/mol).

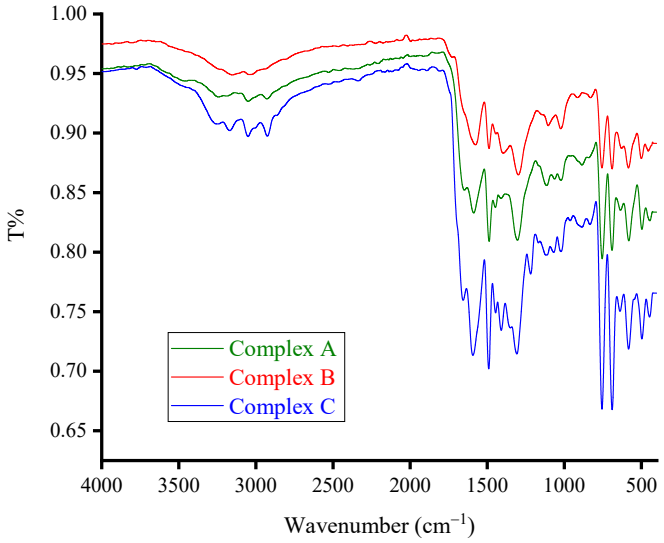

Figure 2. The FT-IR spectra of complex A, complex B, and complex C.

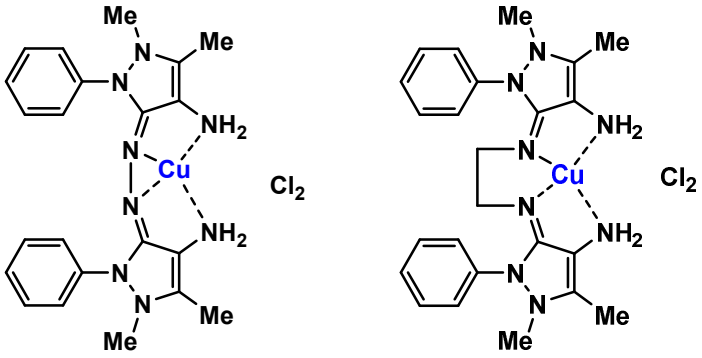

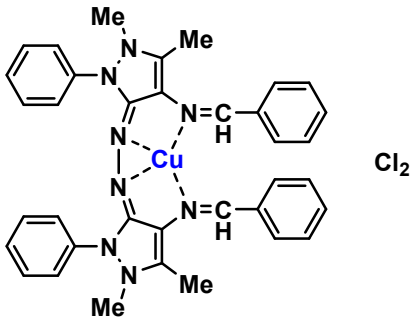

Figure 3. Proposed chemical structures of the synthesized copper(II) complexes.

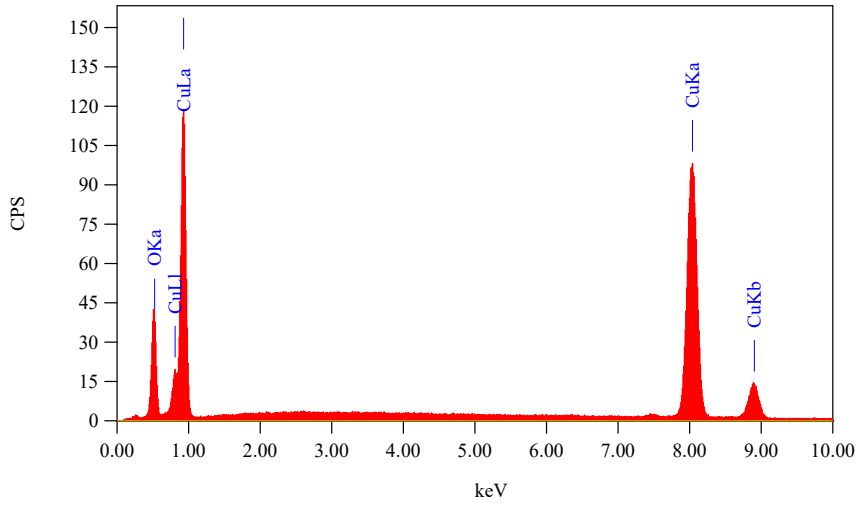

Figure 4a. EDX spectrum of oxide A generated from the thermal decomposition of complex A.

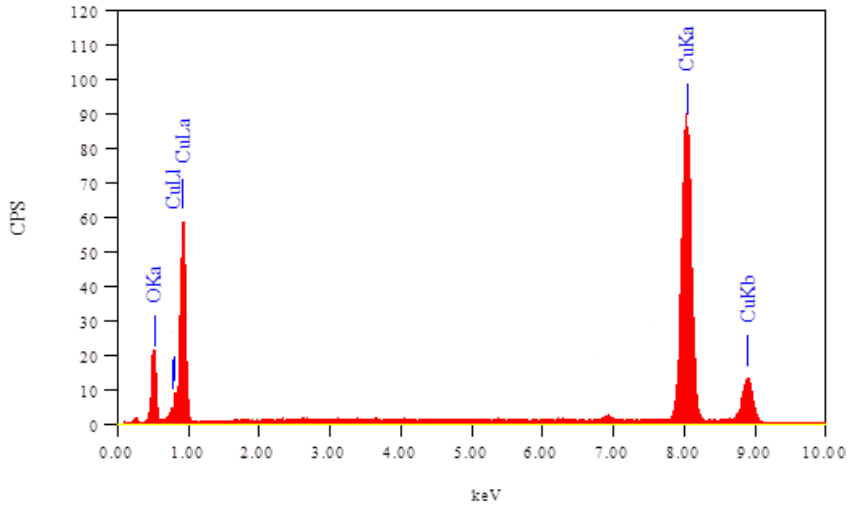

Figure 4b. EDX spectrum of oxide B generated from the thermal decomposition of complex B.

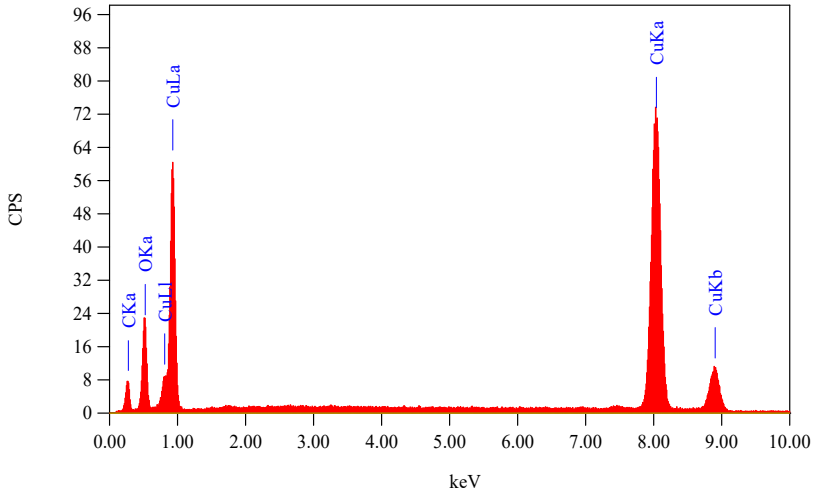

Figure 4c. EDX spectrum of oxide C generated from the thermal decomposition of complex C.

SEM data

Four SEM micrographs of oxide A, oxide B, and oxide C were captured at multiple magnifications and are presented in Figures 5, 6, and 7, respectively. Oxide A and oxide B exhibit similar surface topology, while oxide C displays a slightly different morphology, possibly due to the presence of carbons in the sample. Oxide A and oxide B are composed of individual particles with a cubic-like shape. Most of these particles have six faces, although there are also particles with multiple faces. Upon closer examination in the magnified images (2,500× and 5,000×), the particle faces

appear smooth, and some particles exhibit sharp edges. In the case of oxide A, the particles are densely packed together, forming three-dimensional branches that extend in various directions, creating clear gaps between them. Conversely, in oxide B, the particles are closely accumulated in two-dimensional directions, forming large individual plates with no distinct gaps. The particles of oxide C do not exhibit a clearly defined cubic structure. Instead, they have a texture resembling stones, with varying shapes and sizes. These stone-like particles are irregularly stacked on top of each other, resulting in the formation of aggregates with gaps between them. The SEM micrographs showed that the particle size diameters for oxide A were in the range 10-20 μm, for oxide B were in the range 7-16 μm, and for oxide C were in the range 8-10 μm.

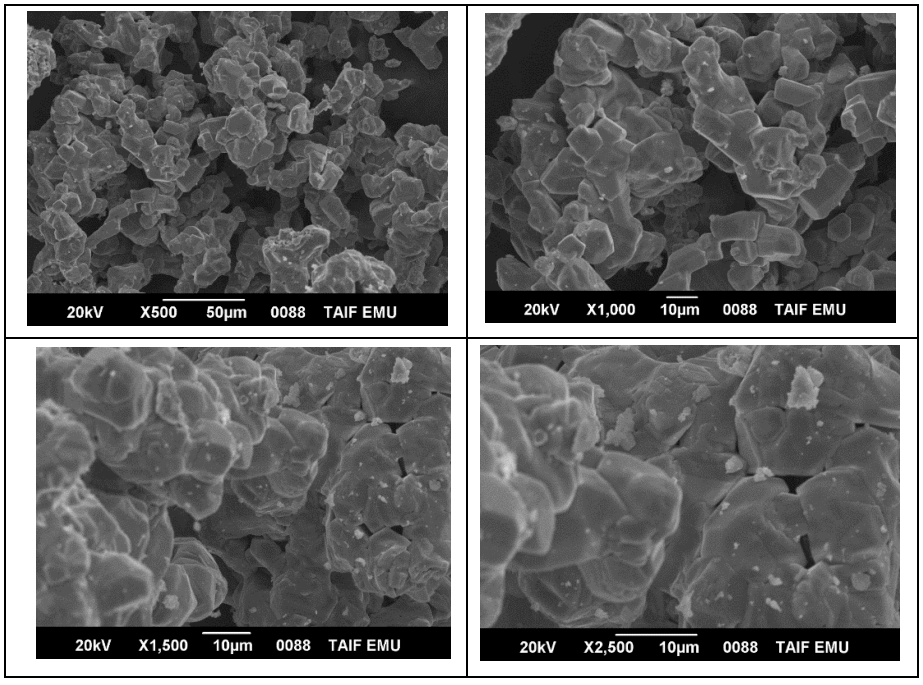

Figure 5. SEM micrographs of oxide A generated from the thermal decomposition of complex A.

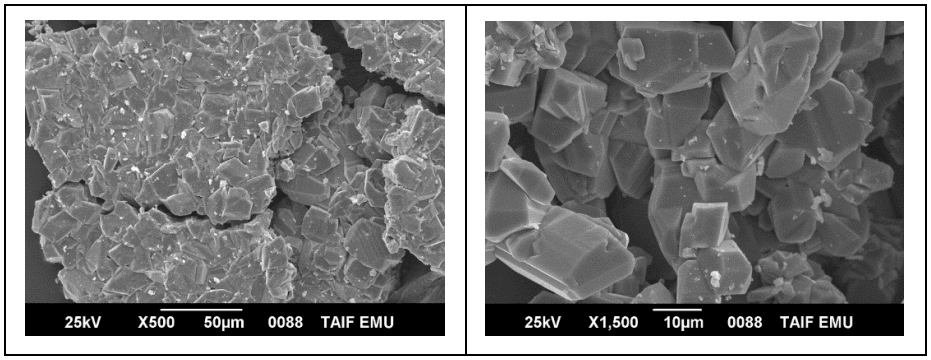

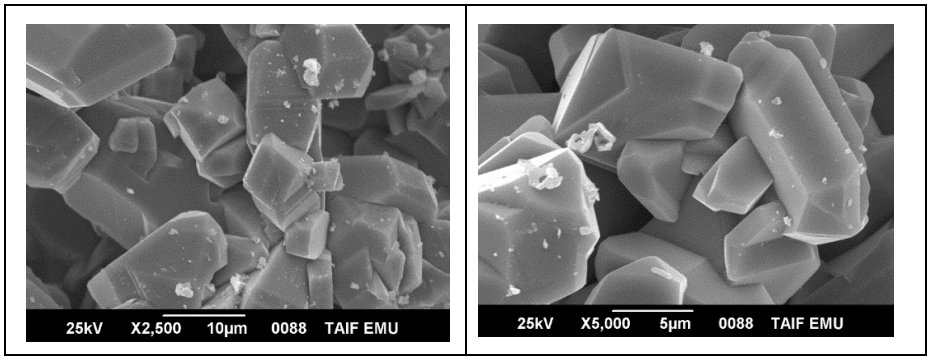

Figure 6. SEM micrographs of oxide B generated from the thermal decomposition of complex B.

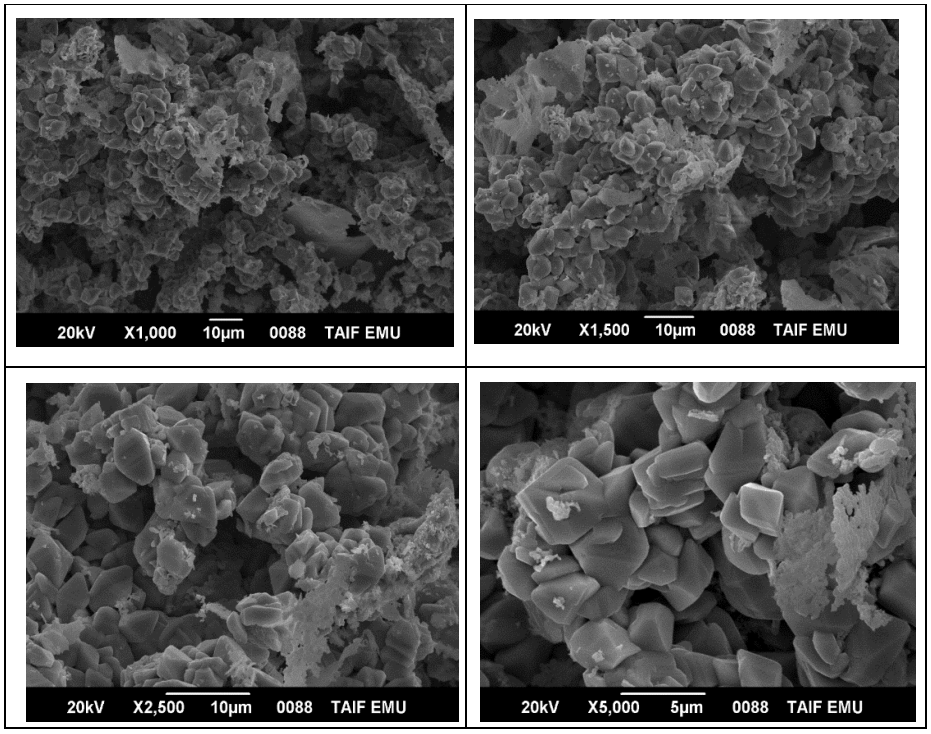

Figure 7. SEM micrographs of oxide C generated from the thermal decomposition of complex C.

FT-IR data

For example, one of the manufactured oxides (oxide A) was scanned by FT-IR spectrometer within the wavenumber range 4000 to 400 cm^{-1}, and the collected spectrum is shown in Figure 8. Oxide A generates one very strong and sharp IR spectral band located at 444 cm^{-1}. This band could be referred to as the ν(Cu-O) vibrations. The oxide also exhibited three very weak

absorption bands at 1575, 1270, and 1000 cm^{-1}. These absorptions may be due to the $\nu(H_2O)$ and $\delta(H_2O)$ vibrations of a few water molecules adsorbed on the CuO surface.

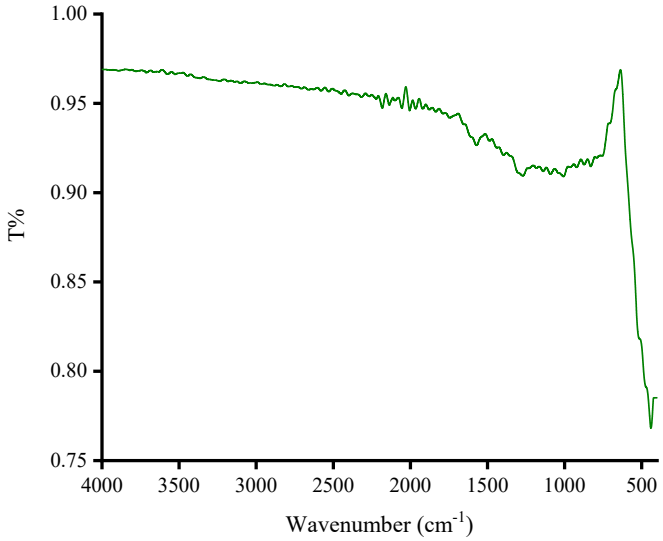

Figure 8. The FT-IR spectrum of oxide A.

CONCLUSION

In this study, we successfully synthesized three Schiff bases based on 4-aminoantipyrine. The synthesized compounds were characterized using FT-IR, ^{1}H, ^{13}C NMR spectra, and elemental analysis, which showed excellent agreement with previously published data. The Schiff base derivatives obtained were ligand A, ligand B, and ligand C. These ligands exhibit interesting structures and possess four nitrogen-donating atoms (NNNN) as coordination sites. Therefore, we investigated their ability to capture copper(II) ions from an aqueous solution. The resulting copper(II) complexes derived from ligand A, ligand B, and ligand C were abbreviated as complex A, complex B, and complex C, respectively. In complexes A and B, the ligands coordinated to the copper(II) ions through the four nitrogen atoms (NNNN) of the 4-aminoantipyrine-N and azomethine-N groups, while in complex C, the ligand coordinated to the copper(II) ions using the four azomethine nitrogen atoms. To further analyze the synthesized complexes, we burned complex A, complex B, and complex C at 600 °C for 3 h, resulting in the formation of oxide A, oxide B, and oxide C, respectively. EDX data revealed that oxide C is CuO contaminated with some carbons, whereas oxide A and oxide B are pure CuO. The diameter of oxide A particles ranged from 10 to 20 μm, oxide B particles ranged from 7 to 16 μm, and oxide C particles ranged from 8 to 10 μm.

ACKNOWLEDGMENT

The research was funded by the Princess Nourah bint Abdulrahman University Researchers Supporting Project number (PNURSP2024R134), Princess Nourah bint Abdulrahman University, Riyadh, Saudi Arabia.

REFERENCES

1. Gull, P.; Dar, O.A.; Malik, M.A.; Hashmi, A.A. Design, synthesis, characterization and antimicrobial/antioxidant activities of 1,4-dicarbonyl-phenyl-dihydrazide based macrocyclic ligand and its Cu(II), Co(II) and Ni(II) complexes. *Micro. Pathog.* **2016**, 100, 237-243.
2. Shrivastava, H.Y.; Kanthimathi, M.; Nair, B.U. Copper(II) complex of a tridentate ligand: an artificial metalloprotease for bovine serum albumin. *Biochim. Biophys. Acta* **2002**, 1573, 149-155.
3. Sankar, R.; Manikandan, P.; Malarvizhi, V.; Fathima, T.; Shivashangari, K.S.; Ravikumar, V. Green synthesis of colloidal copper oxide nanoparticles using *Carica papaya* and its application in photocatalytic dye degradation. *Spectrochim. Acta A* **2014**, 121, 746-750.
4. da Silva, C.M.; da Silva, D.; Modolo, L.V.; Alves, R.B.; de Resende, M.A.; Martins, C.V.B.; de Fátima, Â. Schiff bases: A short review of their antimicrobial activities. *J. Adv. Res.* **2011**, 2, 1-8.
5. Singh, P.; Quraishi, M.A. Corrosion inhibition of mild steel using Novel Bis Schiff's Bases as corrosion inhibitors: Electrochemical and Surface measurement. *Measurement* **2016**, 86, 114-124.
6. El-Boraey, H.A. Structural and thermal studies of some aroylhydrazone Schiff's bases-transition metal complexes. *J. Therm. Anal. Calorim.* **2005**, 81, 339-346.
7. Aghera, V.K.; Parsania, P.H. Effect of substituents on thermal behavior of some symmetric double schiff's bases containing a cardo group. *J. Sci. Ind. Res.* **2008**, 67, 1083-1087.
8. Paulpandiyan, R.; Raman, N. DNA binding propensity and nuclease efficacy of biosensitive Schiff base complexes containing pyrazolone moiety: Synthesis and characterization. *J. Mol. Struct.* **2016**, 1125, 374-382.
9. Zhang, S.J.; Li, H.; Gong, C.L.; Wang, J.Z.; Wu, Z.Y.; Wang, F. Novel 4,5-diazafluorene-based Schiff base derivatives as Al^{3+} ions fluorescence turn-on sensors. *Synth. Met.* **2016**, 217, 37-42.
10. Ejidike, I.P.; Ajibade, P.A. Synthesis, characterization and biological studies of metal(II) complexes of (3E)-3-[(2-{(E)-[1-(2,4-dihydroxyphenyl) ethylidene]amino}ethyl)imino]-1-phenylbutan-1-one Schiff Base. *Molecules* **2015**, 20, 9788-9802.
11. Mahmoud, M.A.; Zaitone, S.A.; Ammar, A.M.; Sallam, S.A. Synthesis, structure and antidiabetic activity of chromium(III) complexes of metformin Schiff-bases. *J. Mol. Struct.* **2016**, 1108, 60-70.
12. Abou Melha, K.S.A.; Al-Hazmi, G.A.A.; Refat, M.S. Synthesis of nano-metric gold complexes with new Schiff bases derived from 4-aminoantipyrene, their structures and anticancer activity. *Russ. J. Gen. Chem.* **2017**, 87, 3043-3051.
13. Naglah, A.M.; Al-Omar, M.A.; Kalmouch, A.; Gobouri, A.A.; Abdel-Hafez, S.H.; El-Megharbel, S.M.; Refat, M.S. Synthesis, spectroscopy, and anticancer activity of two new nanoscale Au(III) N4 Schiff base complexes. *Russ. J. Gen. Chem.* **2019**, 89, 1702-1706.
14. Alibrahim, K.A.; Al-Fawzan, F.F.; Refat, M.S. Chemical preparation of nanostructures of Ni(II), Pd(II), and Ru(III) oxides by thermal decomposition of new metallic 4-aminoantipyrine derivatives. catalytic activity of the oxides. *Russ. J. Gen. Chem.* **2019**, 89, 2528-2533.
15. Alibrahim, K.A.; Al-Fawzan, F.F.; Refat, M.S. Synthesize palladium and nickel oxide nanoparticles in the presence of 4-aminoantipyrine derivative as a precursor: Decolorization efficiency of methylene blue. *Rev. Roum. Chim.* **2020**, 65, 343-352.
16. Nakamoto, K. *Infrared Spectra of Inorganic and Coordination Compounds*. Willey: New York; **1970**.